RSC Advances

ROYAL SOCIETY OF CHEMISTRY

www.rsc.org/advances

Graphical Abstract

RSC Advances

Articles

An effective quaternary nano-sized Er^{3+}:$Y_3Al_5O_{12}$/Pt-PdS/ZnS visible-light photocatalyst for H_2 production

Chunxiao Lu[a], Yang Chen[a], Yun Li[a], Chunhong Ma[a], Hongbo Zhang[a], Yuwei Guo[a,b], and Jun Wang[a,*]

[a] *Colloge of Chemistry, Liaoning University, Shenyang 110036, P.R. China*

[b] *Department of Chemistry, Baotou Normal College, Baotou 014030, P.R. China*

As a novel visible-light photocatalyst, the Er^{3+}:$Y_3Al_5O_{12}$, Pt and PdS (as dual co-catalysts) decorated ZnS nanocatalysts (Er^{3+}:$Y_3Al_5O_{12}$/Pt-PdS/ZnS) were fabricated by deposition-precipitation and ultrasonic dispersion methods. The visible-light photocatalytic H_2 production activity of prepared Er^{3+}:$Y_3Al_5O_{12}$/Pt-PdS/ZnS was evaluated by using Na_2S and Na_2SO_3 as sacrificial reagents in aqueous solution under a 300 W xenon lamp irradiation. For Pt-PdS/ZnS system, the Er^{3+}:$Y_3Al_5O_{12}$ can effectively improve the visible-light photocatalytic activity of ZnS. Er^{3+}:$Y_3Al_5O_{12}$/Pt-PdS/ZnS with 0.13 wt % PdS, 0.3 wt % Pt contents and 0.30:1.00 mass ratio shows the highest photocatalytic H_2 production activity in the sulfide/sulfite (0.2 mol/L Na_2S and 0.3 mol/L Na_2SO_3) aqueous solution as sacrificial reagents.

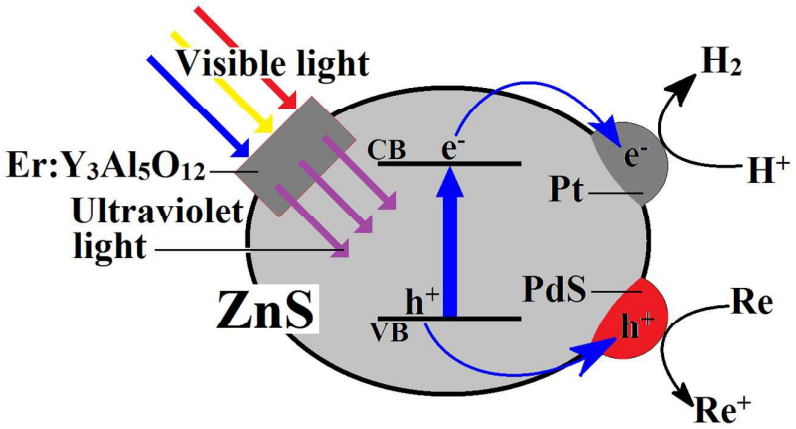

RSC Advances

RSCPublishing

ARTICLE

An effective quaternary nano-sized Er^{3+}:$Y_3Al_5O_{12}$/Pt-PdS/ZnS visible-light photocatalyst for H_2 production

Cite this: DOI: 10.1039/x0xx00000x

Chunxiao Lu[a], Yang Chen[a], Yun Li[a], Chunhong Ma[a], Hongbo Zhang[a], Yuwei Guo[a,b], and Jun Wang[a,*]

Received 00th January 2015,
Accepted 00th January 2015

DOI: 10.1039/x0xx00000x

www.rsc.org/

A high effective and stable up-conversion luminescence agent, Er^{3+}:$Y_3Al_5O_{12}$, was synthesized by sol-gel and calcination methods. And then, as a novel visible-light photocatalyst, the Er^{3+}:$Y_3Al_5O_{12}$, Pt and PdS (as dual co-catalysts) decorated ZnS nano-sized composite, Er^{3+}:$Y_3Al_5O_{12}$/Pt-PdS/ZnS, were fabricated by deposition-precipitation and ultrasonic dispersion methods. All prepared samples were characterized by X-ray diffractometer (XRD), scanning electron microscopy (SEM), transmission electron microscopy (TEM), X-ray photoelectron spectroscopy (XPS) and energy dispersive X-ray spectroscopy (EDX). UV-vis absorption and PL spectra of Er^{3+}:$Y_3Al_5O_{12}$ were also determined. The visible-light photocatalytic H_2 production activity of prepared Er^{3+}:$Y_3Al_5O_{12}$/Pt-PdS/ZnS was evaluated by using Na_2S and Na_2SO_3 as sacrificial reagents in aqueous solution under a 300 W xenon lamp irradiation. In addition, some influence factors such as Er^{3+}:$Y_3Al_5O_{12}$ and ZnS mass ratio, catalyst amount, irradiation time and irradiation intensity on visible-light photocatalytic H_2 production of Er^{3+}:$Y_3Al_5O_{12}$/Pt-PdS/ZnS were investigated in detail. It was found that the Er^{3+}:$Y_3Al_5O_{12}$ can effectively improve the visible-light photocatalytic activity of ZnS. Particularly, Er^{3+}:$Y_3Al_5O_{12}$/Pt-PdS/ZnS with 0.13 wt % PdS and 0.3 wt % Pt contents and 0.30:1.00 mass ratio shows the highest photocatalytic H_2 production activity in the sulfide/sulfite (0.2 mol/L Na_2S and 0.3 mol/L Na_2SO_3) aqueous solution as sacrificial reagents.

1. Introduction

With the increasing human activities, fossil fuels, which have caused many serious environmental problems, are difficult to maintain the growing energy demand. Therefore, a clean and sustainable energy of the future has aroused extensive attention. Hydrogen, the cleanest fuel, is expected to surpass the fossil fuels.[1-4] In particular, photocatalytic H_2 production from water splitting using semiconductor photocatalysts has drawn considerable attention as a promising way of resolving energy and environmental problems.[5-7]

Since the Honda-Fujishima effect was first reported,[8] many kinds of photocatalysts for the water decomposition have been developed by many researchers. Recently, metal sulfides have been intensively studied as active photocatalysts due to their unique catalytic functions.[9-13] Among them, the wide band gap (ca. 3.6 eV) of ZnS photocatalyst exhibits rapid generation of electron-hole pairs upon photoexcitation and highly negative reduction potentials of excited electrons. However, owing to relatively wide band gap, it can be activated mainly under ultraviolet-light which accounts for less than 5.0 % of the solar light energy reaching the Earth's surface and therefore imposes restrictions on the application of ZnS photocatalysts.[14-16] To obtain higher activity for photocatalytic H_2 production from water splitting by ZnS, much more techniques have been used, for example, addition of sacrificial agents,[17,18] surface modification of photocatalysts, doping of metal or nonmetal ions,[19,20] semiconductor coupling.[21,22] These methods are proved to be effective, but, they reduce the catalytic activity of ZnS itself. It is the best way to maintain the catalytic activity of the wide band gap of ZnS and meet the energy needs. Recently, in our researches a new improved method was proposed, that is, some photocatalysts are combined with up-conversion luminescence agent to improve photocatalytic H_2 production from water splitting.

We emphasize a solely photonics approach to enhance the photocatalytic activity: a blue shift by up-conversion luminescence agent with the ability to transform visible-light into ultraviolet-light, which satisfy the requirements of large band-gap semiconductor materials. During the past decades, up-conversion luminescence agent, which can convert longer wavelength radiation to shorter wavelength fluorescence via a two-photon or multi-photon mechanism, have attracted a tremendous amount of attention, for example, Yb^{3+}/Er^{3+}:$NaGdF_4$, Yb^{3+}/Er^{3+}:YVO_4 and Er^{3+}:$Y_3Al_5O_{12}$ etc., have been reported.[23-25] Among them, Er^{3+}:$Y_3Al_5O_{12}$ was deemed to be a most efficient visible-to-ultraviolet up-conversion luminescence agent, which can effectively activate the ZnS to carry out visible-light photocatalytic reaction.

So far, the efficiency of photocatalytic H_2 production from water splitting is still low. A key reason is that the photogenerated electrons/holes are easily consumed via recombination. In order to promote the rapid surface transfer of photogenerated electrons and holes from photocatalyst, the widely used strategy for achieving this purpose is loading co-catalysts. During the past few years, various co-catalysts have been reported to be utilized on photocatalyst, such as Pt, MoS_2, RuO_2 and PdS, whereas the role of the co-catalysts in the reaction is not the same. Pt and MoS_2 are effective reduction co-catalysts (RCs), while PdS and RuO_2 are effective oxidation cocatalysts (OCs). They are proved to be beneficial for the efficient

charge separation and surface reactions, which achieve a higher efficiency of photocatalytic H_2 production from water splitting. So, the use of dual co-catalysts may be crucial for improve the photocatalytic activity.[26-30]

Herein, an effective and stable up-conversion luminescence agent, Er^{3+}:$Y_3Al_5O_{12}$, was synthesized by sol-gel method and the nano-sized ZnS particles were obtained by hydrothermal method. And then, a novel visible-light photocatalyst, Er^{3+}:$Y_3Al_5O_{12}$/Pt-PdS/ZnS, was successfully prepared by deposition and calcination methods. The experimental results showed that the photocatalytic H_2 production activity of ZnS could be significantly enhanced by the presence of Er^{3+}:$Y_3Al_5O_{12}$ and by supported Pt and PdS as dual co-catalyst. How the Er^{3+}:$Y_3Al_5O_{12}$ affects the prepared nano-sized Pt-PdS/ZnS particles for visible-light photocatalytic H_2 production activity was also investigated in detail. In addition, the mechanism of up conversion luminescence process of Er^{3+}:$Y_3Al_5O_{12}$ and the excitation principle of Er^{3+}:$Y_3Al_5O_{12}$/Pt-PdS/ZnS photocatalysts under visible-light irradiation were proposed.

2. Experimental procedure

2.1. Materials and reagents

Erbium oxide (Er_2O_3, 99.999 %), yttrium oxide (Y_2O_3, 99.999 %) and aluminum nitrate nonahydrate ($(AlNO_3)_3·9H_2O$, analytical pure), citric acid ($C_6H_8O_7$, analytical pure) and nitric acid (HNO_3, 65 %, analytical pure, Veking Company, China) were used to synthesize the up-conversion luminescence agent (Er^{3+}:$Y_3Al_5O_{12}$). Zinc acetate dihydrate ($C_4H_6O_4Zn·2H_2O$, 99 %, Sinopharm Chemical Reagent Co., Ltd, China), dodecyl sodium sulfate ($C_{12}H_{25}NaO_4S$, chemically pure, Sinopharm Chemical Reagent Co., Ltd, China) and sodium sulfide nonahydrate ($Na_2S·9H_2O$, 98 %, Aladdin Industrial Corporation, China) were used to synthesize the nano-sized ZnS particles. Hexachloroplatinic acid hexahydrate ($H_2PtCl_6·6H_2O$, 97 %, Sinopharm Chemical Regent Co., Ltd, China) and palladium chloride ($PdCl_2$, analytical pure, Sinopharm Chemical Reagent Co., Ltd, China) were used as dual co-catalysts precursor. Sodium sulfite anhydrous (Na_2SO_3, 97 %, Sinopharm Chemical Regent Co., Ltd, China) and sodium sulfide nonahydrate ($Na_2S·9H_2O$, 98 %, Sinopharm Chemical Regent Co., Ltd, China) were dissolved with double distilled water (Millipore Corporation, USA) as sacrificial agent. All chemicals were used without further purification.

2.2. Synthesis of up-conversion luminescence agent (Er^{3+}:$Y_3Al_5O_{12}$)

The up-conversion luminescence agent, Er^{3+}:$Y_3Al_5O_{12}$, was synthesized by a nitrate-citrate sol-gel and calcination ways.[31,32] At the beginning, $Y(NO_3)_3$ and $Er(NO_3)_3$ solutions were planted by dissolving Y_2O_3 (0.01 mol, 2.2715 g) and Er_2O_3 (3.34×10^{-5} mol, 0.0128 g) into suitable hot HNO_3 solution (about 60 °C), respectively. The planted $Y(NO_3)_3$ and $Er(NO_3)_3$ solutions were put together with $Al(NO_3)_3·9H_2O$ (0.0336 mol, 12.6208 g) while stirring magnetically, and the homogenous solution was acquired. Then, the solid citric acid (0.1680 mol, 33.9351 g) was also put into the mentioned mixture solution (mol ratio of citric acid: metal ion is 3:1). The solution was continued to be stirred and heated at 50-60 °C until the transparent sol was triumphantly come into being. And then, the transparent sol was heated at 80 °C for 24 h and became the gel. After the gel cooled in the air, it was ground into good homogeneous powders. For the sake of removing residual organic components and nitrate ions the powders were heated at 1100 °C for 2.0 h in a muffle furnace. In the end, the sintered substance was removed and permitted to cool down to the room temperature in atmosphere. Whereupon, the white Er^{3+}:$Y_3Al_5O_{12}$ particles were acquired.

2.3. Preparation of visible-light photocatalyst (Er^{3+}:$Y_3Al_5O_{12}$/Pt-PdS/ZnS)

ZnS nanospheres were prepared using hydrothermal method.[33-35] At first, sodium dodecylsulfate (0.3 g) was added to the distilled water (25 mL) to form a solution. $Zn(acac)_2$ (1.76 g) was dissolved in the above solution slowly. Subsequently, Na_2S (0.4 mol/L, 20 mL) was added dropwise to the mixture under stirring magnetically for 60 min, and then added different mass ratios of the above prepared Er^{3+}:$Y_3Al_5O_{12}$. The as-formed solution was transferred into Teflon lined stainless steel autoclave (100 mL) and maintained at 160 °C for 2.0 h. After cooling to room temperature naturally, a white suspension was separated by centrifugation, washed with distilled water and ethanol several times, and then dried at 60 °C in a vacuum.

Modification of Er^{3+}:$Y_3Al_5O_{12}$/ZnS with PdS (0.13 wt %) and Pt (0.30 wt %) as dual co-catalysts was realized by deposition-precipitation of PdS and then ultrasonic dispersion and liquid boiling method of Pt.[36-38] The photocatalysts were prepared by following two procedures: firstly, a $PdCl_2$ aqueous solution (0.0011 mol/L) was added dropwise to a suspension of Er^{3+}:$Y_3Al_5O_{12}$/ZnS powder (1.0 g, as prepared above) dispersed in Na_2S aqueous solution (0.5 mol/L) under stirring magnetically. After centrifugation, washed thoroughly with water and dried at 60 °C for 10 h, H_2PtCl_6 aqueous solution was added to a suspension of Er^{3+}:$Y_3Al_5O_{12}$/PdS-ZnS dispersed in H_2O (10 mL). The suspension was heated to boiling point and kept constant temperature for 15 min. After centrifugation, washed thoroughly with water until Cl^- was below detection, and dried at 60 °C for 12 h. The obtained powders were calcined in vacuum at 200 °C for 3.0 h. Finally, the Er^{3+}:$Y_3Al_5O_{12}$/Pt-PdS/ZnS photocatalysts were obtained. For the purpose of comparison, Pt-PdS/ZnS were also prepared in the same way.

2.4. Analytical method

The prepared Er^{3+}:$Y_3Al_5O_{12}$, Pt-PdS/ZnS and Er^{3+}:$Y_3Al_5O_{12}$/Pt-PdS/ZnS were characterized by powder X-ray diffraction (XRD, D-8, Bruker-axs, Germany) using Ni filtered Cu κα radiation in the range of 2θ from 10° to 70°), scanning electron microscopy (SEM, JEOL JSM-5610LV, Hitachi Corporation, Japan), transmission electron microscopy (TEM, JEOL JEM2100, Hitachi Corporation, Japan), energy dispersive X-ray spectroscopy (EDX, JEOL JSM-5610LV, Hitachi Corporation, Japan), X-ray photoelectron spectroscopy (XPS, Escalab 250XI, Thermo, America), UV-vis absorption spectra (UV-2450, Shimadzu, Japan) and PL spectra (RF-5301PC, Shimadzu, Japan).

2.5. Visible-light photocatalytic H_2 production experimental

The photocatalytic H_2 production experiments were performed in a 500 mL Pyrex reactor at ambient temperature and atmospheric pressure. The headspace of the reactor was connected to an inverted burette which is filled with water, allowing the measurement of the evolved hydrogen gas. In a typical photocatalytic experiment, Er^{3+}:$Y_3Al_5O_{12}$/Pt-PdS-ZnS powder as photocatalysts was dispersed under constant stirring in an aqueous solution containing 0.20 mol/L Na_2S and 0.30 mol/L Na_2SO_3. Before irradiation, the system was bubbled with argon for 30 min to remove the dissolved air inside in order to ensure the reaction system was under an anaerobic condition. Then, the suspensions were irradiated for 5.0 h using a 300 W xenon lamp (LX-300, Deruifeng hardware electrical

appliance businesses, China) applied as light source, which was positioned on the side of photoreactor. The irradiation wavelength was controlled by a combination of a cold mirror (CM-1) and a water filter ($350 < \lambda < 800$ nm). For visible-light irradiation, a cut off filter (L42) was fitted to the aforementioned light source ($400 < \lambda < 800$ nm). The formation of hydrogen was confirmed by injecting 0.50 mL of the reactor headspace gas in a gas chromatograph (GC-8A, MS-5A column, TCD, Ar Carrier, Shimadazu, Japan).

3. Results and discussions

3.1. XRD, SEM, TEM, EDX and XPS of prepared $Er^{3+}:Y_3Al_5O_{12}$/Pt-PdS/ZnS

Fig. 1 shows XRD patterns of synthesized $Er^{3+}:Y_3Al_5O_{12}$ up-conversion luminescence agent and prepared Pt-PdS/ZnS and $Er^{3+}:Y_3Al_5O_{12}$/Pt-PdS/ZnS photocatalysts. The $Er^{3+}:Y_3Al_5O_{12}$ (**Fig. 1(a)**) was identified according to JCPDS #33-0040 file of $Y_3Al_5O_{12}$. It demonstrated that we had well synthesized the $Er^{3+}:Y_3Al_5O_{12}$, in which the Er^{3+} ions entered the crystal lattice, taking the place of the partial Y^{3+} ion. As shown in **Fig. 1(b)**, three pronounced peaks at 28.6° (111), 47.5° (220) and 56.3° (311) in sample can be indexed to the cubic sphalerite ZnS (JCPDS # 05-0566), and no impurity peaks are observed. The broad diffraction peaks of ZnS are due to its small crystallite size. **Fig. 1(d, e** and **f)** shows the characteristic peaks of both cubic sphalerite ZnS and $Er^{3+}:Y_3Al_5O_{12}$. From these XRD patterns, we can see the main five peaks at $2\theta = 18.12°$ (211), 33.36° (400), 42.58° (422), 46.62° (521) and 55.12 °(532) corresponding to the $Er^{3+}:Y_3Al_5O_{12}$, suggesting that the $Er^{3+}:Y_3Al_5O_{12}$ part exists in these samples. These patterns of ZnS and $Er^{3+}:Y_3Al_5O_{12}$ consist of two sets of diffraction peaks, and the broadening peaks match well with ZnS. And yet the intensity of all diffraction peaks of $Er^{3+}:Y_3Al_5O_{12}$ in $Er^{3+}:Y_3Al_5O_{12}$/Pt-PdS/ZnS powder weakens obviously as against that of pure $Er^{3+}:Y_3Al_5O_{12}$ powder. The characteristic diffraction peaks of Pt and PdS from **Fig. 1(c, d, e** and **f)** reveal that only 0.30 wt % Pt and 0.13 wt % PdS loaded on the surface of ZnS nanocrystals are not enough to produce the characteristic peaks in XRD patterns.

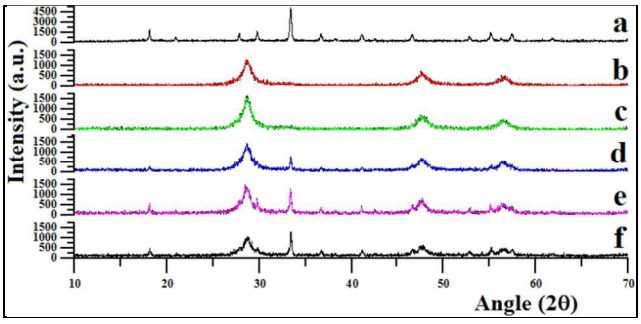

Fig. 1 The XRD patterns of (a) $Er^{3+}:Y_3Al_5O_{12}$ (heat-treated at 1100 °C for 120 min), (b) ZnS and (c-f) $Er^{3+}:Y_3Al_5O_{12}$/Pt-PdS/ZnS (0.13 wt % PdS and 0.3 wt % Pt contents and different $Er^{3+}:Y_3Al_5O_{12}$ and ZnS mass ratios ((c) 0.00:1.00, (d) 0.15:1.00, (e) 0.30:1.00 and (f) 0.45:1.00)).

Fig. 2 displays typical SEM image for $Er^{3+}:Y_3Al_5O_{12}$ (**Fig. 2(a)**), Pt-PdS/ZnS (**Fig. 2(b)**) and $Er^{3+}:Y_3Al_5O_{12}$/Pt-PdS/ZnS (**Fig. 2(c)**). From the image of $Er^{3+}:Y_3Al_5O_{12}$ depicted in **Fig. 2(a)**, numerous homogeneous sphere shaped particles can be seen clearly. The image **Fig. 2(b)** shows monodispersed irregular spheres with an average diameter of ca. 50 nm, confirming the ZnS nanospheres, while the surfaces of the nanospheres are loaded with numerous particles of diameter less than 5 nm. These particles can be verified as PdS and Pt nanoparticles. Both particles are dispersed on the surface of ZnS. As shown in **Fig. 2(c)**, the size of particles is different, among them most of the particles' is about 50 nm. However, there are not some slightly greater particles which can be regarded as the $Er^{3+}:Y_3Al_5O_{12}$ (**Fig. 2(a)**. Because the structure of $Er^{3+}:Y_3Al_5O_{12}$ is loose, after the treatment of ultrasound grind and boil it can be covered on the surface of ZnS. These findings justify that the $Er^{3+}:Y_3Al_5O_{12}$ has been merged with ZnS. In addition, the PdS and Pt have also been stored on them.

Fig. 2(d) shows the TEM of $Er^{3+}:Y_3Al_5O_{12}$/Pt-PdS/ZnS photocatalyst. It can be seen that the ZnS displays the slightly regular shape with the average diameter of about 50 nm. Besides, PdS and Pt nanoparticles as cocatalysts are randomly dispersed on the surface of ZnS particles. The typical particle sizes of Pt and PdS are estimated to be ca. 3-5 nm and 10-15 nm, respectively. Particularly, some nanoparticles with a diameter around 15-20 nm are $Er^{3+}:Y_3Al_5O_{12}$, which are dispersedly deposited on the surface of ZnS particles.

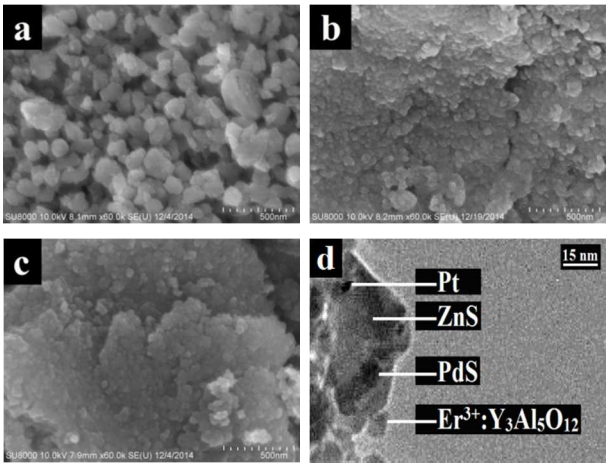

Fig. 2 The SEM images of (a) $Er^{3+}:Y_3Al_5O_{12}$ (heat-treated at 1100 °C for 120 min), (b) Pt-PdS/ZnS (0.13 wt % PdS and 0.3 wt % Pt contents) and (c) $Er^{3+}:Y_3Al_5O_{12}$/Pt-PdS/ZnS (0.13 wt % PdS and 0.3 wt % Pt contents and 0.30:1.00 $Er^{3+}:Y_3Al_5O_{12}$ and ZnS mass ratio) and TEM image of (d) $Er^{3+}:Y_3Al_5O_{12}$/Pt-PdS/ZnS (0.13 wt % PdS and 0.3 wt % Pt contents and 0.30:1.00 $Er^{3+}:Y_3Al_5O_{12}$ and ZnS mass ratio).

As shown in **Fig. 3**, the composition of the as-prepared products is confirmed by energy-dispersive X-ray spectroscopy (EDX) analysis. As displayed in **Fig. 3(a)**, the results of EDX analysis show that the peaks of Er, Y, Al, and O elements are observed without any other peaks and the atomic ratio of Y, Al, and O is close to 3:5:12, which is in agreement with the stoichiometric ratio of $Er^{3+}:Y_3Al_5O_{12}$. The **Fig. 3(b)** shows that the products predominantly contain Zn and S elements, with a tiny amount of Pt and Pd (Pt and Pd signals arose from depositing small amounts of Pt and PdS on the ZnS). The **Fig. 3(c)** also indicate that Er, Y, Al, O, Zn, S, Pt and Pd elements are coexisting in the quaternary catalyst close to the stoichiometric ratio further confirming successful fabrication of $Er^{3+}:Y_3Al_5O_{12}$/Pt-PdS/ZnS. These results were consistent with the XRD pattern presented above simultaneously.

XPS spectra of $Er^{3+}:Y_3Al_5O_{12}$/Pt-PdS/ZnS photocatalyst is shown in **Fig. 4**. It indicates that this photocatalyst contains Zn, S, Pt, Pd, Er, Y, Al and O elements and the corresponding peaks are plotted carefully. The **Fig. 4** shows that the characteristic peaks of Zn (1046 eV $2p_{1/2}$ and 1023 eV $2p_{3/2}$) and S (163eV $2p_{3/2}$ and 227eV 2s) can be clearly observed in the wide scan spectrum and as shown in **Fig.4 (a** and **b)**, the binding energy peaks located at 73 eV, 75 eV,

337 eV and 340 eV well match with the reported values of Pt $4f_{5/2}$, Pt $4f_{7/2}$, Pd $3d_{5/2}$ and Pd $3d_{3/2}$ XPS peaks.[39,40] These implied that Pt and PdS were successfully decorated on ZnS. Besides these characteristic peaks, the figure also presents other peaks at 173 eV (Er $4d_{5/2}$), 294 eV (Y $3p_{3/2}$), 147 eV (Y $3d_{3/2}$), 118 eV (Al 2s), 91 eV (Al $2p_{3/2,1/2}$), 531 eV (O 1s) and 24 eV (O 2s), which closely agree with the composition of Er^{3+}:$Y_3Al_5O_{12}$. All peaks of the photocatalyst emerge with a slightly shift due to the efficient charge transfer between the adjacent components during the photocatalytic reaction.

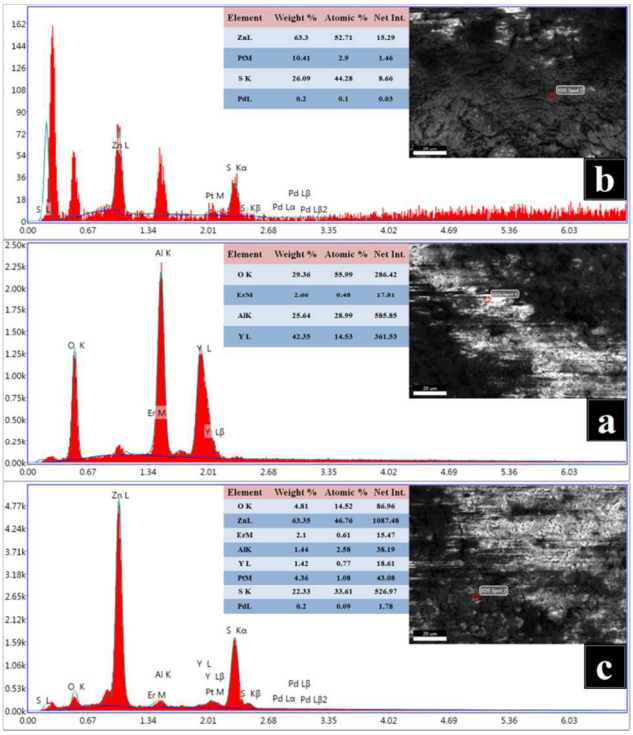

Fig. 3 The EDX patterns of (a) Er^{3+}:$Y_3Al_5O_{12}$ (heat-treated at 1100 °C for 120 min), (b) Pt-PdS/ZnS (0.13 wt % PdS and 0.3 wt % Pt contents) and (c) Er^{3+}:$Y_3Al_5O_{12}$/Pt-PdS/ZnS (0.13 wt % PdS and 0.3 wt % Pt contents and 0.30:1.00 Er^{3+}:$Y_3Al_5O_{12}$ and ZnS mass ratio).

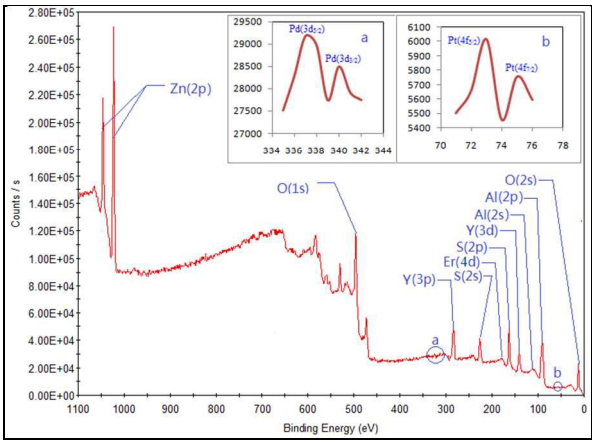

Fig. 4 XPS spectra of Er^{3+}:$Y_3Al_5O_{12}$/Pt-PdS/ZnS (0.13 wt % PdS and 0.3 wt % Pt contents and 0.30:1.00 Er^{3+}:$Y_3Al_5O_{12}$ and ZnS mass ratio).

The absorption and PL spectra of up-conversion luminescence agent Er^{3+}:$Y_3Al_5O_{12}$ are illustrated in **Fig. 5**. From the **Fig. 5(a)**, it can be seen that three typical peaks located at 410 nm, 524 nm, 653 nm in absorption spectra. **Fig. 5 (b, c** and **d)** shows the PL spectra of Er^{3+}:$Y_3Al_5O_{12}$ under the excitation wavelengths of 410 nm, 524 nm and 653 nm, respectively, where the absorption peaks can be obviously found in the absorption spectra. The emission peaks are conspicuous in the ultraviolet-light region (250-400 nm). Therefore, it can be confirmed that the Er^{3+}:$Y_3Al_5O_{12}$ as up-conversion luminescence agent can absorb the visible lights and emit the ultraviolet lights. These findings prove that the ZnS combined with Er^{3+}:$Y_3Al_5O_{12}$ will be activated effectively by visible light to enhance the effect of photocatalytic H_2 production.

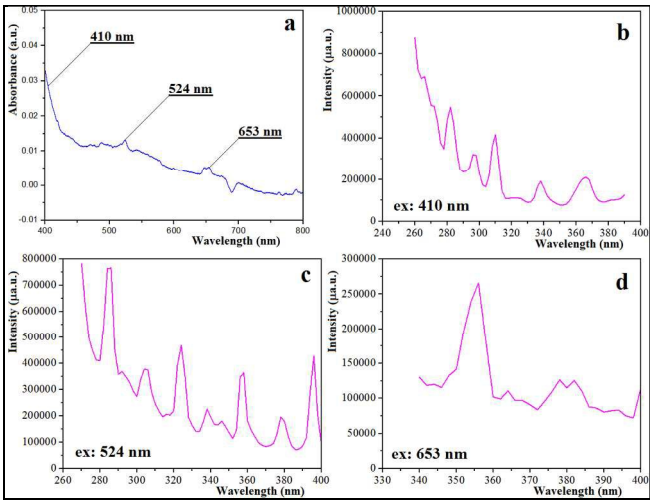

Fig. 5 Absorption spectrum (a) and PL spectra (b-d) of Er^{3+}:$Y_3Al_5O_{12}$ (heat-treated at 1100 °C for 120 min) at various excitation wavelengths.

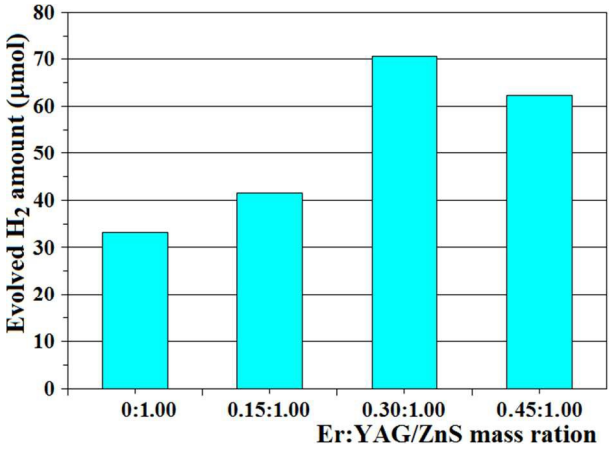

Fig. 6 Influence of Er^{3+}:$Y_3Al_5O_{12}$ and ZnS mass ratios on visible-light photocatalytic H_2 production activity of Er^{3+}:$Y_3Al_5O_{12}$/Pt-PdS/ZnS (0.13 wt % PdS and 0.3 wt % Pt contents). (0.20 g/L catalyst, 0.2 mol/L Na_2S, 0.3 mol/L Na_2SO_3, 300 W xenon lamp. Er:YAG: Er^{3+}:$Y_3Al_5O_{12}$.)

3.2. The influence of Er^{3+}:$Y_3Al_5O_{12}$ and ZnS mass ratio on visible-light photocatalytic H_2 production activity of Er^{3+}:$Y_3Al_5O_{12}$/Pt-PdS/ZnS

In preliminary experiments, the study of the influence of the amount of up-conversion luminescence agent (Er^{3+}:$Y_3Al_5O_{12}$) in the system was performed in order to optimize the conditions of visible-light photocatalytic H_2 production. The results are presented in **Fig. 6**. It shows that the effects of Er^{3+}:$Y_3Al_5O_{12}$ amount on the photocatalytic

activity of the Er^{3+}:$Y_3Al_5O_{12}$/Pt-PdS/ZnS photocatalysts. The amount of the photocatalytic H_2 production continues to enhance with an increase of Er^{3+}:$Y_3Al_5O_{12}$ amount (from 0:1.00 mass ratio to 0.30:1.00 mass ratio) in the Er^{3+}:$Y_3Al_5O_{12}$/Pt-PdS/ZnS photocatalysts, and then it decreases with the further increase of Er^{3+}:$Y_3Al_5O_{12}$ amount (0.45:1.00 mass ratio). All of the Er^{3+}:$Y_3Al_5O_{12}$/Pt-PdS/ZnS photocatalysts present higher photocatalytic H_2 production rate than that over Pt-PdS/ZnS, revealing that the Er^{3+}:$Y_3Al_5O_{12}$ amount affects largely the photocatalytic activity of Pt-PdS/ZnS. The appropriate increase of Er^{3+}:$Y_3Al_5O_{12}$ amount can offer much more ultraviolet-light to activate ZnS, which results in the increase of the amount of photocatalytic H_2 production. However, the further increase of Er^{3+}:$Y_3Al_5O_{12}$ amount relatively leads to the decrease of the amount of photocatalytic H_2 production due to the fact that the active surface of ZnS nanospheres decreases.

3.3. The influence of photocatalyst amount on visible-light photocatalytic H_2 production of Er^{3+}:$Y_3Al_5O_{12}$/Pt-PdS/ZnS and Pt-PdS/ZnS

Fig. 7 shows the influence of the amount of photocatalysts on the rate of visible-light photocatalytic H_2 evolution of Er^{3+}:$Y_3Al_5O_{12}$/Pt-PdS/ZnS. It can be found that, at begining, the amounts of H_2 evolution increase along with the increase of amount for both Er^{3+}:$Y_3Al_5O_{12}$/Pt-PdS/ZnS and Pt-PdS/ZnS photocatalysts up to a certain weight (0.20 g/L), and then become a sharply decrease with further increase of catalyst amounts. Maybe, it is due to the fact that no more photons could be absorbed to carry out the photocatalytic H_2 evolution, because of scattering and reflection of lights caused by overmuch catalyst particles. All in all, the reason is the combination effect of thermodynamic and kinetic factors of the photoelectron generation and transfer in photocatalytic reactions. An optimal amount of photocatalysts is required in order to attain the highest photocatalytic H_2 evolution efficiency.

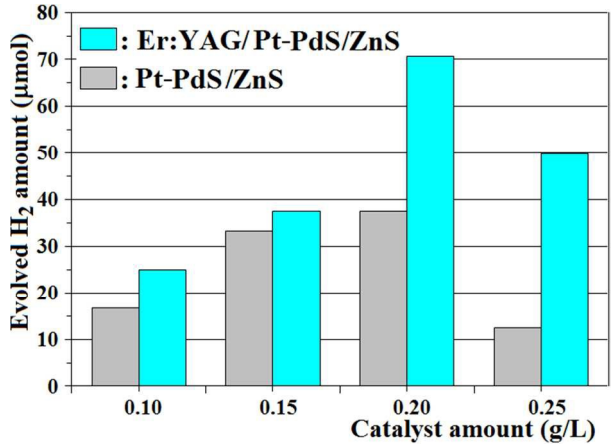

Fig. 7 Influence of the catalyst amounts on visible-light photocatalytic H_2 production activity of Pt-PdS/ZnS (0.13 wt % PdS and 0.3 wt % Pt contents) and Er^{3+}:$Y_3Al_5O_{12}$/Pt-PdS/ZnS (0.13 wt % PdS and 0.3 wt % Pt contents and 0.30:1.00 Er^{3+}:$Y_3Al_5O_{12}$ and ZnS mass ratio). (0.2 mol/L Na_2S, 0.3 mol/L Na_2SO_3, 300 W xenon lamp. Er:YAG: Er^{3+}:$Y_3Al_5O_{12}$.)

3.4. Photocatalytic activity comparison of Er^{3+}:$Y_3Al_5O_{12}$/Pt-PdS/ZnS and Pt-PdS/ZnS in visible-light photocatalytic H_2 production

Fig. 8 shows the comparison of H_2 production amounts catalysed by Er^{3+}:$Y_3Al_5O_{12}$/Pt-PdS/ZnS and Pt-PdS/ZnS along with visible-light irradiation time. It can be found that, obviously, the amounts of H_2 evolution both significantly increase with the lengthening of visible-light irradiation time for two photocatalysts. However, the amount by using Er^{3+}:$Y_3Al_5O_{12}$/Pt-PdS/ZnS is much more than that by using Pt-PdS/ZnS at any visible-light irradiation time. It can be considered that, because of the presence of Er^{3+}:$Y_3Al_5O_{12}$ possessing up-conversion luminescence effect from visible-light to ultraviolet-light, it can provide more ultraviolet-light to stimulate ZnS to carry out the photocatalytic H_2 production. It reveals that the presence of Er^{3+}:$Y_3Al_5O_{12}$ could dramatically improve the visible-light photocatalytic H_2 production activity of the Pt-PdS/ZnS catalysts.

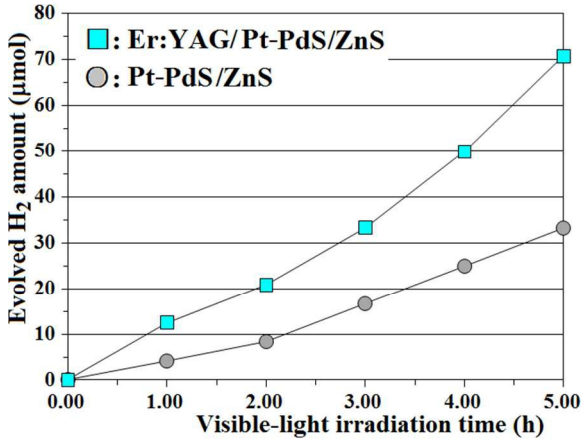

Fig. 8 Influence of irradiation time on visible-light photocatalytic H_2 production activity of Pt-PdS/ZnS (0.13 wt % PdS and 0.3 wt % Pt contents) and Er^{3+}:$Y_3Al_5O_{12}$/Pt-PdS/ZnS (0.13 wt % PdS and 0.3 wt % Pt contents and 0.30:1.00 Er^{3+}:$Y_3Al_5O_{12}$ and ZnS mass ratio). (0.20 g/L catalyst, 0.2 mol/L Na_2S, 0.3 mol/L Na_2SO_3, 300 W xenon lamp. Er:YAG: Er^{3+}:$Y_3Al_5O_{12}$.)

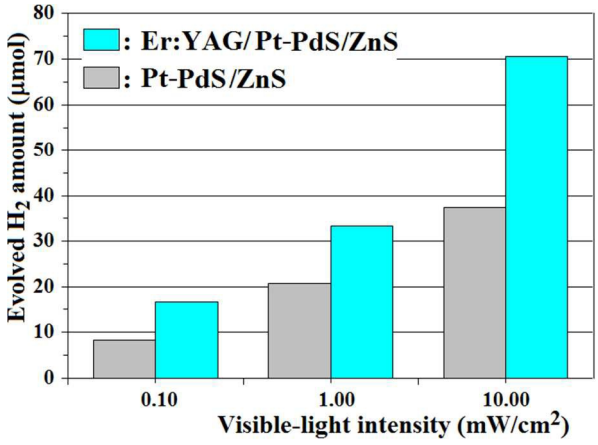

Fig. 9 Influence of irradiation intensity on visible-light photocatalytic H_2 production activity of Pt-PdS/ZnS (0.13 wt % PdS and 0.3 wt % Pt contents) and Er^{3+}:$Y_3Al_5O_{12}$/Pt-PdS/ZnS (0.13 wt % PdS and 0.3 wt % Pt contents and 0.30:1.00 Er^{3+}:$Y_3Al_5O_{12}$ and ZnS mass ratio). (0.20 g/L catalyst, 0.2 mol/L Na_2S, 0.3 mol/L Na_2SO_3, 300 W xenon lamp. Er:YAG: Er^{3+}:$Y_3Al_5O_{12}$.)

3.5. The influence of visible-light irradiation intensity on photocatalytic H_2 production effect of Er^{3+}:$Y_3Al_5O_{12}$/Pt-PdS/ZnS

In this section, the impact of the irradiation intensity on the visible-light photocatalytic H_2 production of Er^{3+}:$Y_3Al_5O_{12}$/Pt-PdS/ZnS is studied and the corresponding data are presented in **Fig. 9**. It can be found that the amounts of H_2 production both dramatically increase

along with the increase of visible-light irradiation intensity for Er^{3+}:$Y_3Al_5O_{12}$/Pt-PdS/ZnS and Pt-PdS/ZnS. It indicates that the high-intensity visible-light irradiation is beneficial to the photocatalytic H_2 production of Er^{3+}:$Y_3Al_5O_{12}$/Pt-PdS/ZnS and Pt-PdS/ZnS. Of course, under the same intensity visible-light irradiation the amounts of H_2 production of Er^{3+}:$Y_3Al_5O_{12}$/Pt-PdS/ZnS photocatalyst is much more than that of Pt-PdS/ZnS powder. It may be attributed to the fact that the Er^{3+}:$Y_3Al_5O_{12}$ offers more ultraviolet-light to ZnS.

3.6. Possible visible-light photocatalytic H_2 production mechanism and process

Based on the above results, a proposed mechanism for visible-light photocatalytic H_2 production from aqueous solution by Er^{3+}:$Y_3Al_5O_{12}$/Pt-PdS/ZnS is illustrated in **Fig. 10**. Firstly, ZnS as a wide band gap photocatalyst plays important role in the photocatalytic H_2 production reaction. In addition, two main reasons for the increase in the photocatalytic activity of Er^{3+}:$Y_3Al_5O_{12}$/Pt-PdS/ZnS were (1) the presence of up-conversion luminescence agent (Er^{3+}:$Y_3Al_5O_{12}$), and (2) the effect of Pt and PdS acting as co-catalyst. The two factors might generate synergistic effect for the enhancement of photocatalytic activity of ZnS. The followings are the detailed interpretation of the main reasons.

(1) The up-conversion luminescence agent (Er^{3+}:$Y_3Al_5O_{12}$) absorbs the visible-light, and then continuously emits the ultraviolet-light. The Er^{3+} ion has abundant energy levels in the ultraviolet range, which allows a variety of up-conversion to occur through absorption of low energy photons by an already excited Er^{3+} ion. Besides, two excited Er^{3+} ions can exchange energy, such that one of the ions is further excited to an even higher energy state, while the other relaxes to a lower state. That is to say, the up-conversion process can be achieved through the chains of ground state absorption (GSA) and excited state absorption (ESA).[41,42] Therefore, under continuous excitation of visible-light, the Er^{3+}:$Y_3Al_5O_{12}$ emits the ultraviolet-light, which can effectively excite ZnS to generate electron-hole pairs.

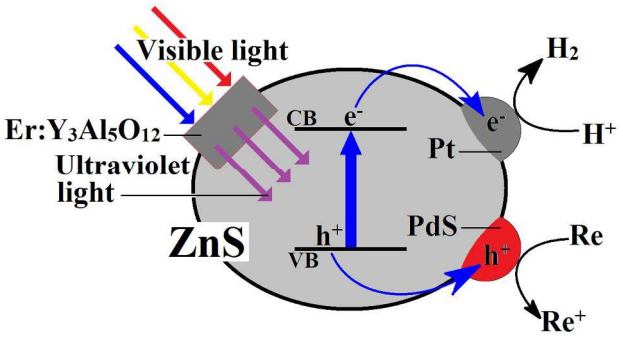

Fig. 10 The schematic diagram of photocatalytic H_2 production over quaternary Er^{3+}:$Y_3Al_5O_{12}$/Pt-PdS/ZnS photocatalysts under visible-light irradiation.

(2) ZnS coloaded with Pt and PdS shows considerably synergistic effect on the photocatalytic H_2 production. Upon ultraviolet-light excitation, the photogenerated electron and hole are produced in the conduction band (CB) and valence band (VB) of ZnS, respectively. Pt is effective reduction co-catalysts, while PdS is effective oxidation co-catalyst. The electrons and holes can be separated and transfer efficiently for promoting the photocatalytic actibity of ZnS. The holes are consumed by the 0.20 mol/L Na_2S and 0.30 mol/L Na_2SO_3 as sacrificial agent. And then, the electrons will transfer to the surface of ZnS and reduce protons to H_2.

Through these experimental observations, it can be believed that the above two supposed factors are the main reasons that lead to the enhanced activity of the Er^{3+}:$Y_3Al_5O_{12}$/Pt-PdS/ZnS photocatalyst.

Conclusions

In summary, a quaternary photocatalyst (Er^{3+}:$Y_3Al_5O_{12}$/Pt-PdS/ZnS) was successfully prepared by sol-gel and hydrothermal methods. The visible-light photocatalytic H_2 production activity of Er^{3+}:$Y_3Al_5O_{12}$/Pt-PdS/ZnS from aqueous solution containing 0.20 mol/L Na_2S and 0.30 mol/L Na_2SO_3 as sacrificial reagents was evaluated under visible-light irradiation. The results indicated that the visible-light photocatalytic H_2 production activity of ZnS can be significantly enhanced in the presence of the up-conversion luminescence agent (Er^{3+}:$Y_3Al_5O_{12}$). Moreover, the loading of Pt and PdS, as reduction and oxidation co-catalysts, respectively, can help the separation and transfer of photogenerated electrons and holes in ZnS for photocatalytic reactions, significantly promoting the visible-light photocatalytic activity. The visible-light photocatalytic activity of prepared Er^{3+}:$Y_3Al_5O_{12}$/Pt-PdS/ZnS is related to the mass ratio of Er^{3+}:$Y_3Al_5O_{12}$ and ZnS, catalyst amount and irradiation intensity. Notably, it is the first time to use quaternary composite compound as an effective and stable photocatalyst for H_2 production, which provides new insight to enhance the photocatalytic H_2 production activity under solar light.

Acknowledgements

The authors greatly acknowledge the National Science Foundation of China (21371084), Innovation Team Project of Education Department of Liaoning Province (LT2012001), Public Research Fund Project of Science and Technology Department of Liaoning Province (2012004001), Shenyang Science and Technology Plan Project (F12-277-1-15 and F13-289-1-00) and Science Foundation of Liaoning Provincial Education Department (L2011007) for financial support. The authors also thank our colleagues and other students for their participating in this work.

Notes and references

[a] *Colloge of Chemistry, Liaoning University, Shenyang 110036, P.R. China.*
[b] *Department of Chemistry, Baotou Normal College, Baotou 014030, P.R. China.*
E-mail: wangjun888tg@126.com, wangjun891@sina.com;
Fax: +86 24 62202053; Tel: +86 24 62207861

1 R. D. Cortright, R. R. Davda and J. A. Dumesic, *Nature*, 2002, **418**, 964-967.
2 Z. Y. Shen, G. Chen, Q. Wang, Y. G. Yu, C. Zhou and Y. Wang, *Nanoscale*, 2012, **4**, 2010-2017.
3 Y. P. Xie, Z. B. Yu, G. Liu, X. L. Ma and H. M. Cheng, *Energ. Environ. Sci.*, 2014, **7**, 1895-1901.
4 N. Z. Bao, L. M. Shen, T. Takata and K. Domen, *Chem. Mater.*, 2008, **20**, 110-117.
5 T. P. Xie, C. L. Liu, L. J. Xu, J. Yang and W. Zhou, *J. Phys. Chem. C*, 2013, **117**, 24601-24610.
6 Y. T. Lu, D. D. Wang, P. Yang, Y. K. Du and C. Lu, *Catal. Sci. Technol.*, 2014, **4**, 2650-2657.
7 X. B. Chen, S. H. Shen, L. J. Guo and S. S. Mao, *Chem. Rev.*, 2010, **110**, 6503-6570.
8 A. Fujishima and K. Honda, *Nature*, 1972, **238**, 37-38.
9 K. Zhang and L. J. Guo, *Catal. Sci. Technol.*, 2013, **3**, 1672-1690.
10 F. Z. Jia , Z. P. Yao and Z. H. Jiang, *Int. J. Hydrgen Energ.*, 2012, **37**,

3048-3055.
11 C. H. Deng, X. Q. Ge, H. M. Hu, L. Yao, C. L Han and D. F. Zhao, *CrystEngComm*, 2014, **16**, 2738-2745.
12 M. Shen, Z. P. Yan, L. Yang, P. W. Du, J. Y. Zhang and B. Xiang, *Chem. Commun.*, 2014, **50**, 15447-15449.
13 S. Martha, D. K. Padhi and K. Parida, *ChemSusChem*, 2014, **7**, 585-597.
14 Y. S. Zhou, G. Chen, Y. G. Yu, Y. J. Feng, Y. Zheng, F. He and Z. H. Han, *Phys. Chem. Chem. Phys.*, 2015, **17**, 1870-1876.
15 A. D. Mani, P. Ghosal and C. Subrahmanyam, *RSC Adv.*, 2014, **4**, 23292-23298.
16 N. X. Li, L. Z. Zhang, J. C. Zhou, D. W. Jing and Y. M. Sun, *Dalton Trans.*, 2014, **43**, 11533-11541.
17 S. J. Hu, L. C. Jia, B. Chi, J. Pu and L. Jian, *J. Power Sources*, 2014, **266**, 304-312.
18 J. L. Yuan, J. Q. Wen, Q. Z. Gao, S. C. Chen, J. M. Li, X. Li and Y. P. Fang, *Dalton Trans.*, 2015, **44**, 1680-1689.
19 J. Zhang, S. W. Liu, J. G. Yu and M. Jaroniec, *J. Mater. Chem.*, 2011, **21**, 14655-14662.
20 J. R. Ran, J. Zhang, J. G. Yu, M. Jaroniec and S. Z. Qiao, *Chem. Soc. Rev.*, 2014, **43**, 7787-7812.
21 S. Liu, X. T. Wang, K. Wang, R. Lv and Y. L. Xu, *Appl. Surf. Sci.*, 2013, **283**, 732-739.
22 Z. Wang, S. W. Cao, S. C. J. Loo and C. Xue, *CrystEngComm*, 2013, **15**, 5688-5693.
23 Z. L. Wang, J. H. Hao and H. L. W. Chan, *J. Mater. Chem.*, 2010, **20**, 3178-3185.
24 F. M. Cheng, K. N. Sun, Y. Zhao, Y. J. Liang, Q. Xin and X. L. Sun, *Ceram. Int.*, 2014, **40**, 11329-11334.
25 J. Zhou, W. X. Zhang, J. Li, B. X. Jiang, W. B. Liu and Y. B. Pan, *Ceram. Int.*, 2010, **36**, 193-197.
26 C. Kong, S. X. Min and G. X. Lu, *Chem. Commun.*, 2014, **50**, 9281-9283.
27 J. Di, J. X. Xia, Y. P. Ge, L. Xu, H. Xu, J. Chen, M. Q. He and H. M. Li, *Dalton Trans.*, 2014, **43**, 15429-15438.
28 M. Barawi, I. J. Ferrer, J. R. Ares and C. Sánchez, *ACS Appl. Mater. Interfaces*, 2014, ***6***, 20544-20549.
29 J. H. Yang, H. J. Yan, X. L. Wang, F. Y. Wen, Z. J. Wang, D. Y. Fan, J. Y. Shi and C. Li, *J. Catal.*, 2012, **290**, 151-157.
30 R. G. Li, H. X. Han, F. X. Zhang, D. G. Wang and C. Li, *Energ. Environ. Sci.*, 2014, **7**, 1369-1376.
31 J. C. Boyer, F. Vetrone, L. A. Cuccia and J. A. Capobianco, *J. Am. Chem. Soc.*, 2006, **128**, 7444-7445.
32 G. J. Feng, S. W. Liu, Z. L. Xiu, Y. Zhang, J. X. Yu, Y. G. Chen, P. Wang and X. J. Yu, *J. Phys. Chem. C*, 2008, **112**, 13692-13699.
33 B. L. Zhu, B. Z. Lin, Y. Zhou, P. Sun, Q. R. Yao, Y. L. Chen and B. F. Gao, *J. Mater. Chem. A*, 2014, **2**, 3819-3827.
34 J. Wang, Y. F. Lim and G. W. Ho, *Nanoscale*, 2014, **6**, 9673-968.
35 J. Y. Zhang, Y. H. Wang, J. Zhang, Z. Lin, F. Huang and J. G. Yu, *ACS Appl. Mater. Interfaces*, 2013, **5**, 1031-1037.
36 H. J. Yan, J. H. Yang, G. J. Ma, G. P. Wu, X. Zong, Z. B. Lei, J. Y. Shi and C. Li, *J. Catal.*, 2009, **266**, 165-168.
37 Y. H. Pai, C. T. Tsai and S. Y. Fang, *J. Power Sources*, 2013, **223**, 107-113.
38 J. L. Meng, Z. M. Yu, Y. Li and Y. D. Li, *Catal. Today*, 2014, **225**, 136-141.
39 Q. Gu, J. L. Long, H. Q. Zhuang, C. Q. Zhang, Y. Q. Zhou and X. X. Wang, *Phys. Chem. Chem. Phys.*, 2014, **16**, 12521-12534.
40 J. Batista, A. Pintar, D. Mandrino, M. Jenko and V. Martin, *Appl. Catal. A: Gen.*, 2001, **206**, 113-124.
41 N. N. Zu, H. G. Yang and Z. W. Dai, *Physica B*, 2008, **403**, 174-177.
42 Z. J. Zhang, W. Z. Wang, J. Xu, M. Shang, J. Ren and S. M. Sun, *Catal. Commun.*, 2011, **13**, 31-34.